Materials Science

http://www.aimspress.com/journal/Materials/

AIMS Materials Science, 3(3): 851-861.
DOI: 10.3934/matersci.2016.3.851
Received: 24 May 2016
Accepted: 27 June 2016
Published: 08 July 2016

Research article

Enhanced thermal conductance of polymer composites through embedding aligned carbon nanofibers

David Wood[1], **Dale K. Hensley**[2], **and Nicholas Roberts**[1,*]

[1] Department of Mechanical and Aerospace Engineering, Utah State University, Old Main Hill, Logan, Utah 84322, USA

[2] Center for Nanophase Materials Sciences, Oak Ridge National Laboratory, Oak Ridge National Laboratory, 1 Bethel Valley Road, Oak Ridge, TN 37831, USA

[*] **Correspondence:** Email: nick.roberts@usu.edu; Tel: +1-435-797-9455.

Abstract: The focus of this work is to find a more efficient method of enhancing the thermal conductance of polymer thin films. This work compares polymer thin films embedded with randomly oriented carbon nanotubes to those with vertically aligned carbon nanofibers. Thin films embedded with carbon nanofibers demonstrated a similar thermal conductance between 40–60 μm and a higher thermal conductance between 25–40 μm than films embedded with carbon nanotubes with similar volume fractions even though carbon nanotubes have a higher thermal conductivity than carbon nanofibers.

Keywords: thermal interface material; thermal conductance; composite; carbon nanofiber; polymer

1. Introduction

Thermal management of microelectronic devices has been a significant challenge for thermal engineers for many decades. The exterior of a processing chip package can exhibit heat fluxes up to 200 W/cm^2 [1]. Poor contact between the exterior of the package and the heat sink due to a micrometer scale surface roughness causes these high heat fluxes to result in very large temperature rises within

the package. Pastes with thermally conductive particles reduce the thermal contact resistance, but due to their low thermal conductivity have not eliminated the thermal bottleneck. The focus of this work is on creating polymer-based materials that exhibit the elastomeric properties desired to eliminate voids while maintaining a high thermal conductivity. This study discusses a more efficient approach to thermal conductance enhancement of polymer films.

Previous studies regarding thermal enhancement of a matrix with a carbon additive have shown additives such as graphene[2–4] and randomly oriented multiwalled carbon nanotubes (CNTs)[5] increase thermal conductivity. This work also focuses on utilizing aligned carbon nanofibers (CNFs) in place of CNTs to achieve a minimal thermal resistance.

Polydimethylsiloxane (Sylgard 184, Dow Corning Corporation) (PDMS) (k = 0.27 W/mK) is used in this study because of its wide spread use in a variety of technologies[6–9]. Previous studies have shown PDMS to be a transparent, non-fluorescent, biocompatible, and nontoxic material that is useful in numerous biomedical applications. Specific examples include a microfluidic interface to electrically and thermally insulate desired components[9, 10], as a porous scaffolding for tissue growth [8], tissue cooling[11, 12], and heat rejection[13]. These same interface properties also make PDMS an ideal material for a thermal interface material (TIM) [14].

Many studies have been conducted to determine the thermal properties of thin film composites used in microelectronic devices [15–27]. Methods include optical thermometry, microcalorimetry, heat flow meter (ASTM E1530), and flash radiometry. A review published by Savija et al. [28] discusses additional analytical and empirical models to estimate thermal resistances.

The most accurate and efficient method to determine a sample's thermal conductivity utilizes a modified ASTM D5470 system. The modified stepped-bar apparatus was originally designed by Thompson et al. [15]. Previous systems based on the standard ASTM D5470 without an oversized TRB have resulted in precise measurements but still contain errors associated with bar misalignment[29]. Even though studies have produced accurate results with the standard 1D reference bar system, measurement accuracy and reproducibility increase dramatically by utilizing an oversized TRB system. Thompson was able to reduce measurement uncertainty with a modified apparatus to nearly 1% in a similar set up to the one employed in this work.

In this work we are performing measurements on flexible substrates under considerable strain (0.5–0.6). A high strain environment is used to reduce contact resistance so as to simplify calculations and to mimic the application environment. A detailed analysis of the effects of strain on PDMS/CNT substrates has previously been conducted by Ralphs et al. [30].

The conventional method to calculate thermal conductivity of a sample uses Fourier's Law in the following form:

$$k = \frac{Qdz}{\Delta T A_c} \tag{1}$$

where ΔT is the temperature difference between the two faces of the sample, Q is the average heat rate through both reference bars, dz is the thickness of the medium, and A_c is the effective contact area between the reference bars and the sample. The cross sectional area of the bottom reference bar (BRB) is used as the effective contact area in the calculations in this study.

The temperature profile through the center line of both reference bars is assumed to be 1D linear conduction, allowing heat fluxes and boundary temperatures to be calculated and extrapolated, respec-

tively, by means of a least squares regression of the temperature data points of each reference bar. The slope of the BRB regression is used to calculate the heat leaving the systems. The average of these slopes can be used in the following equation to determine the thermal conductance of the sample:

$$H = \frac{Q}{\Delta T} \tag{2}$$

where Q is the average of the fitted regression slopes, ΔT is the temperature difference across the sample, and H is the sample thermal conductance.

2. Materials and Method

Figure 1 shows the major steps in the experiment. All films were tested in this manner.

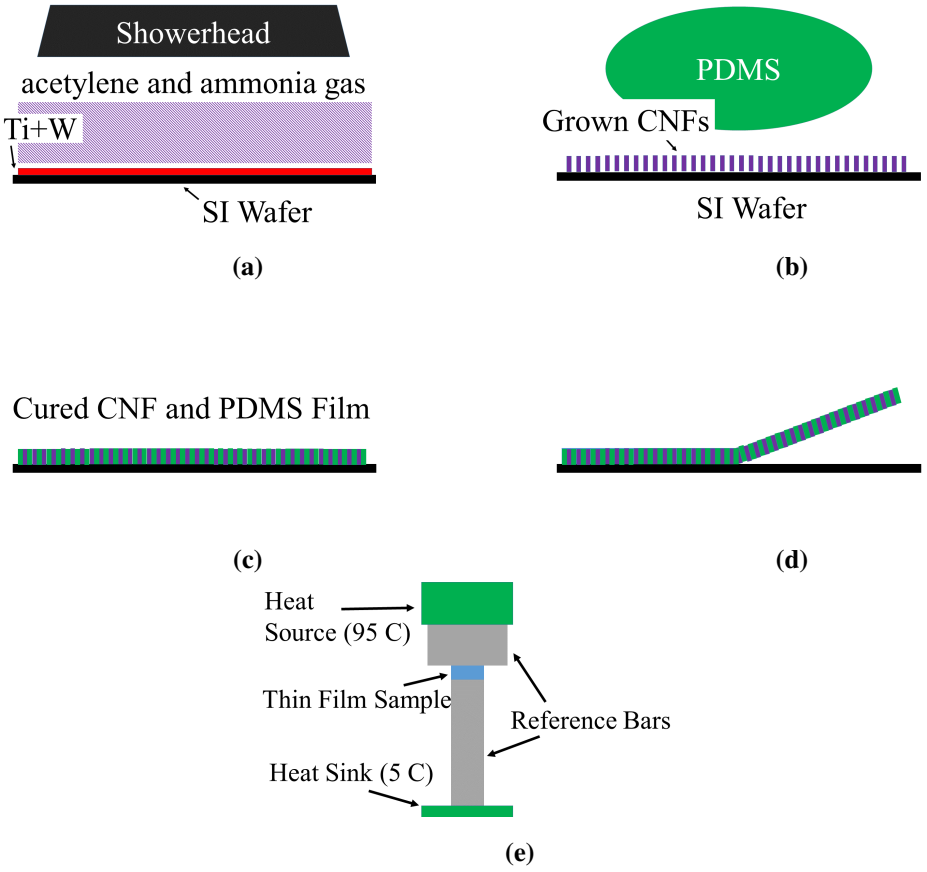

Figure 1. (a) DC-PECVD process to grow VACNFs onto an Si wafer (b) PDMS is spin coated onto a wafer with VACNFs (c) PDMS and VACNFs are cured for 30 minutes at 95°F (d) The cured thin film is removed from Si wafer and prepared for testing (e) Cured thin film is tested in stepped bar apparatus.

2.1. CNF Growth

The vertically aligned carbon nanofibers (VACNFs) were grown using Direct Current (DC) Plasma Enhanced Chemical Vapor Deposition (PECVD). Throughout this DC-PECVD process, the substrate

serves as a cathode and the showerhead as an anode. The VACNF growth is performed in a mixture of acetylene and ammonia gas at several Torr total pressure. The growth process temperature is at 615-825°C. Two different growth regimes were run: slow and fast. The fast growth parameters are 3 amps, 100 sccm of NH_3, 58 sccm of C_2H_2, 10 torr, for 25 minutes. The slow growth parameters are 1 amp, 200 sccm of NH_3, 85 sccm of C_2H_2, 15 torr, for 70 minutes. The substrate is an Si wafer with a thin film of Ti and W (sputtered) to block the etching of the Si wafer so pure carbon fibers can be grown. The Ni (E-Beam evaporated) catalyst is deposited following a photo lithography exposure on a 10μm pitch.

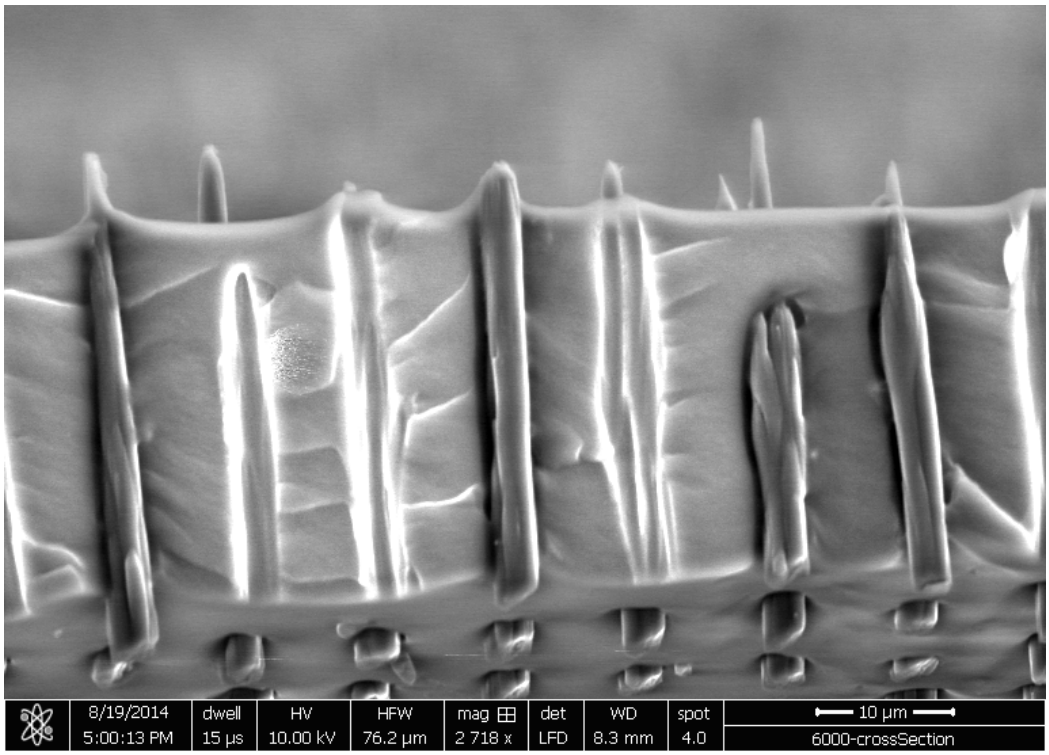

Figure 2. SEM image of CNF/PDMS film.

2.2. CNF/PDMS Films

PDMS is then spun onto the Si+Ti+W substrate in which CNFs have been grown; varying the spin speed and time resulted in various film thicknesses. These thicknesses were chosen as close to the fiber height as possible to ensure that the fibers penetrated both faces of the film. This unobstructed pathway ensures a direct path for thermal energy to pass through the entire film as shown in Figure 2. All PDMS/CNF samples were cured at 95°C for 30 minutes. Figure 3 shows film thickness as a function of spin speed and spin time.

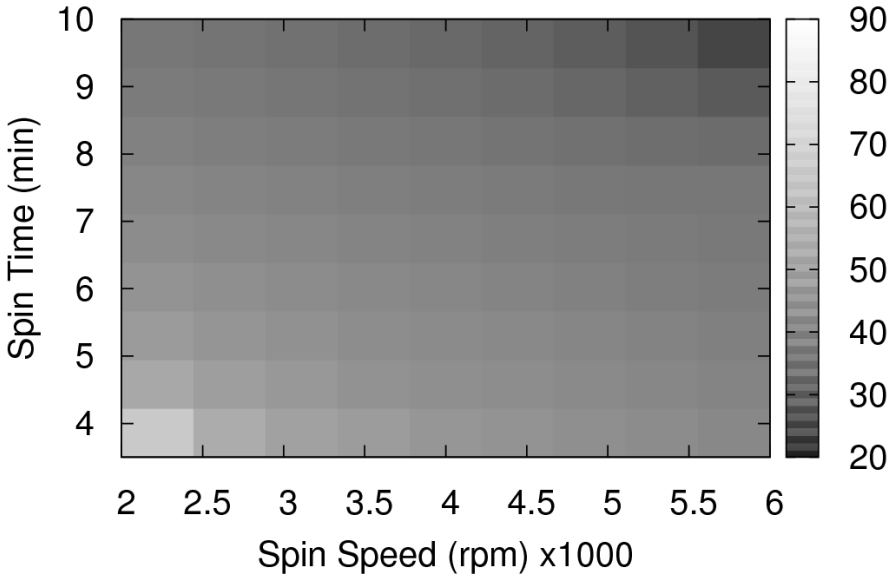

Figure 3. CNF film thickness (μm) with respect to spin speed and time+.

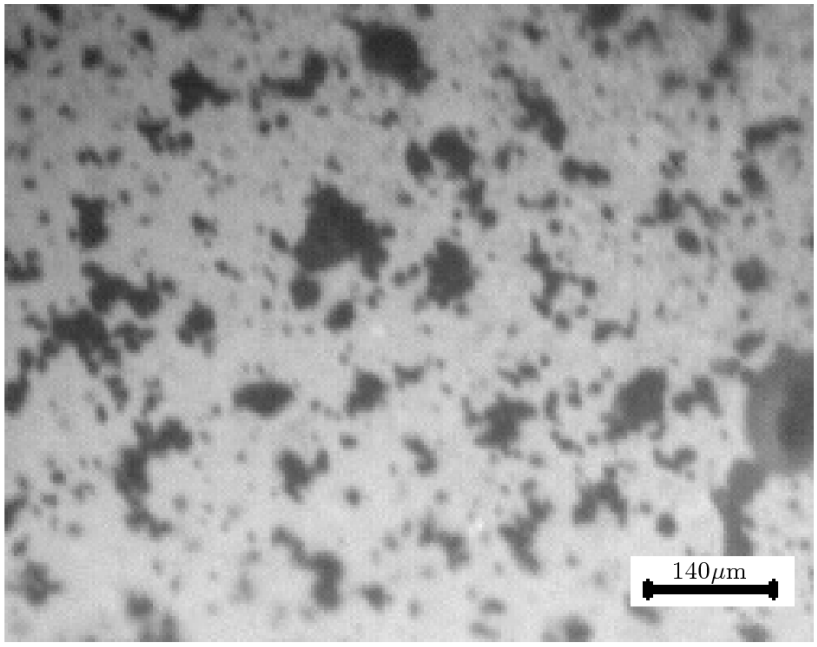

Figure 4. IR image of the CNT film to demonstrate poor dispersion.

2.3. CNT/PDMS Films

CNT segments (Nanostructured and Amorphous Materials, Inc., 50-80 nm dia., 10-20 μm length, 95% purity) are randomly mixed with liquid PDMS then spun and cured onto a wafer together. No measures were taken to evenly disperse the CNTs within the polymer matrix before curing the films as seen in Figure 4. All PDMS/CNT samples were cured at 95°C for 30 minutes. Figure 5 shows how film thickness varies for differing spin speeds and spin times for the PDMS/CNT samples.

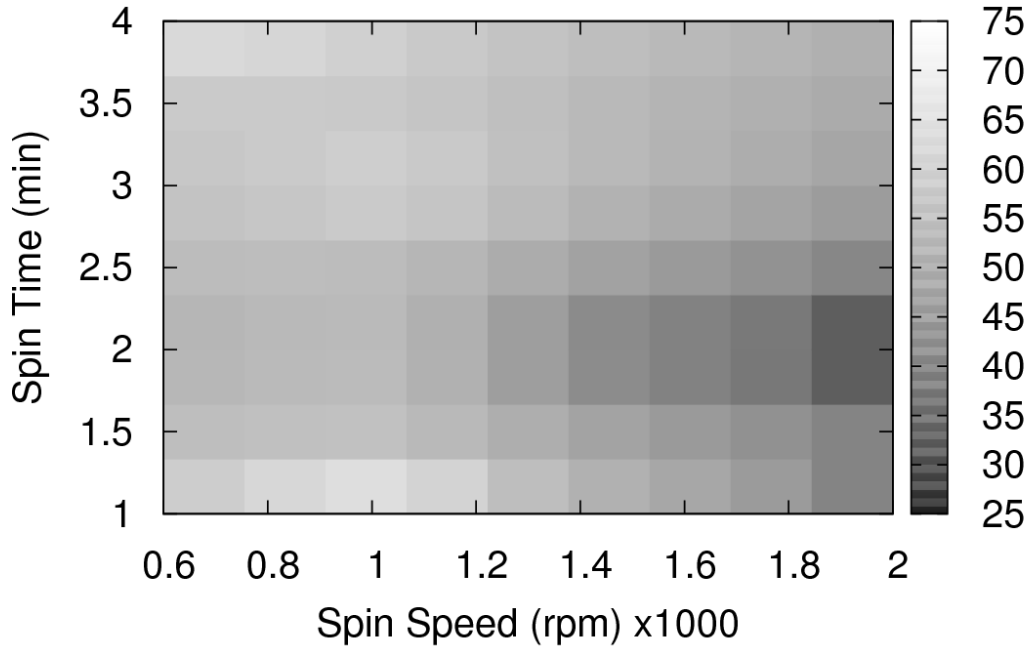

Figure 5. CNT film thickness (μm) with respect to spin speed and time0000.

2.4. Thermal Resistance Measurement

Films are removed from the substrate and tested for their thermal resistance in the stepped bar apparatus. 1D conduction is assumed to simplify calculations. This is justified by an FEA analysis of the ideal insulation conditions against the actual insulation as seen in Figure 6. To create this environment, the reference bars and the sample were heavily insulated on the transverse sides of the bars. The bars were nested in 1 in. outer diameter nylon foam cores and then wrapped in a 2 in. thick fiberglass insulation blanket for additional thermal insulation.

Upper and lower boundary conditions were held constant with heated/cooled copper blocks. The heat source is held at a constant 95°C with a resistance heater. The heat sink is held at 5°C with a circulating cooling bath. Temperature is measured at 16 locations along the center axis of both reference bars, 10 and 6 in the TRB and BRB by precision placed thermocouples, respectively. Data is recorded for fifteen minutes with an Omega 16-channel OMB-DAQ-2416 data acquisition system and $\pm$0.001 K resolution Type-T thermocouples at a sample rate of 0.16 Hz for films enhanced with nanotubes

and nanofibers, respectively. Equation 1 is then used to determine the film thermal resistance. This sample rate is chosen since the system is at steady state conditions and also to negate the effects of small perturbations in the temperature of the reference bars.

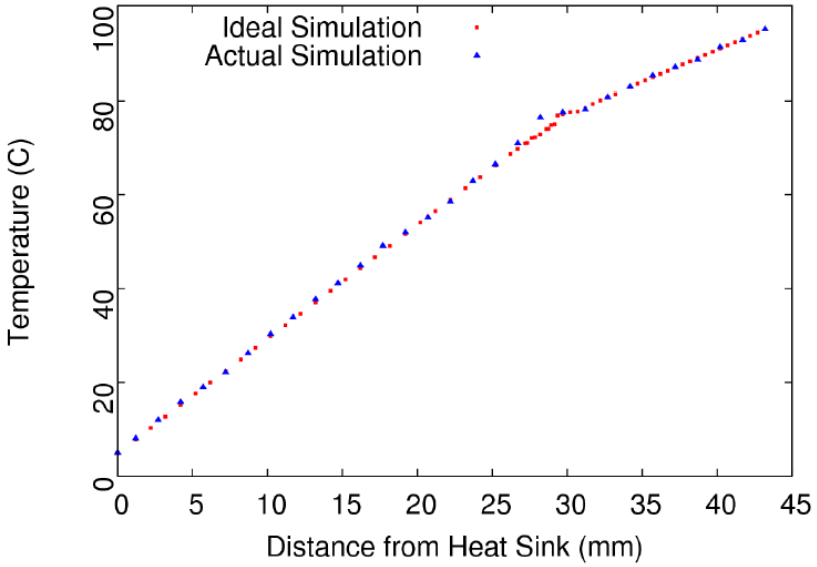

Figure 6. FEA analysis of center line temperatures: ideal vs actual insulation.

The three curves fitted to the data are used to calculate $\frac{dT}{dz}$. Q, related to the slope of the fitted linear curves, is averaged and used in Equation 2.

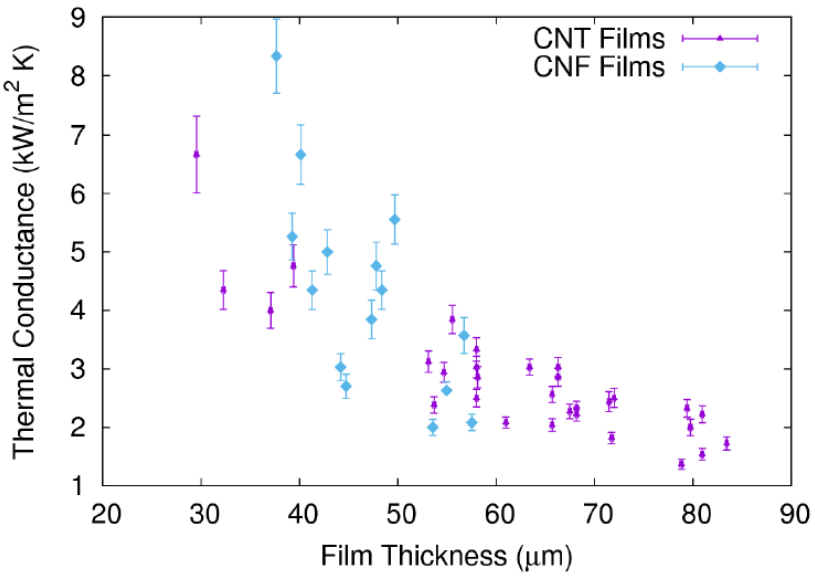

Figure 7. Film Thicknesses vs Measured Conductance.

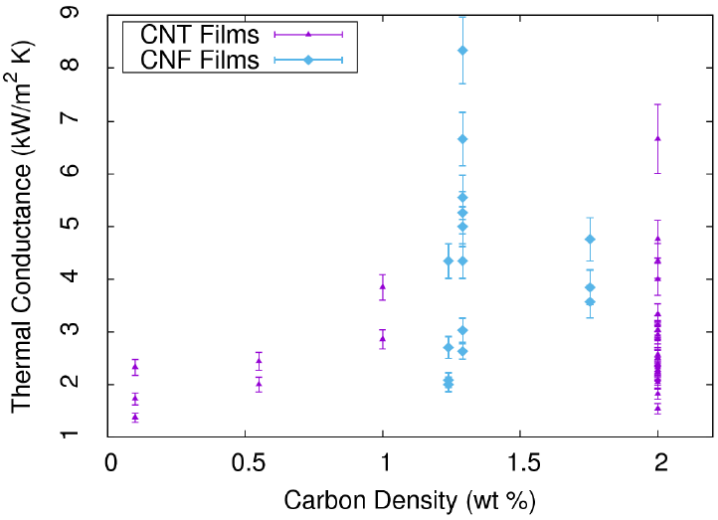

Figure 8. Effect of carbon additive density on film's conductance.

3. Results

As shown in Figure 7, the measured thermal conductance of films enhanced with randomly oriented CNTs ranged from 1.50 to 4.76 kW/m^{2}K between thickness of 30 to 81 μm. Likewise, the aligned CNF enhanced films thermal conductances ranged from 2.00 to 6.66 kW/m^{2}K over thicknesses of 40 to 60 μm. A decreasing thermal conductance is observed with increasing thickness since a conductance is inversely proportional to the film thickness. The linear decrease in thermal conductance with increasing film thickness suggests a near constant thermal conductivity for each the CNT and CNF films.

4. Discussion

Although the films exhibited small thermal resistances they did not entirely remove the thermal contact resistance from the stepped-bar apparatus. The thermal conductances plotted in Figure 7 show the combined total of thermal and contact resistances of the films measured by the apparatus. By testing various thicknesses, the observed contact resistance is considered negligible because the associated uncertainties bounded the graph's origin.

Figure 8 shows thermal conductance as a function of carbon density. Only a minor dependence was observed in the CNT films whereas the CNF films conductances relied heavily on CNF density. Thermal conductance of pure PDMS thin films was observed to be 2.32 kW/m^{2}K at a thickness of 70 μm.

Uncertainty in the tests is measured using the Kline-McClintock formula. Uncertainty from the thermal resistance measurement, u_R, is calculated using the same technique as seen in [15]. Each measurement's total uncertainty is calculated in the equation below:

$$u_{Total} = \sqrt{{u_K}^2 + {u_{stat}}^2 + {u_{design}}^2} \tag{3}$$

where U_K is the uncertainty from the thin film's thermal resistance measurement as seen in [15], u_{stat} is the uncertainty from the variation between individual experiments, and u_{design} is the total design

stage uncertainty from the load cell and DAQ.

Uncertainties arising from the resolution of the camera used to find the sample's thickness are accounted for in u_K.

The variance in the results of samples with the same carbon density are mainly due to the amount of independent variables within the experiment. Parameters such as actual force applied and interface temperatures varied slightly between all experiments which contributed a small amount of uncertainty in the final results.

Using a 95% confidence interval, the average thermal conductance for CNT enhanced films is 3.16 $\pm$ 0.177 kW/m^{2}K and 3.54 $\pm$ 0.327 kW/m^{2}K for CNF enhanced films. Major sources of uncertainty result from the contact resistance between the film and the reference bars, and the DAQ's 16-bit resolution.

5. Conclusion

This study shows that embedded CNTs and CNFs enhance the thermal conductivity of a polymer thin film therefore reducing the thermal resistance. It also shows that vertically aligned CNFs density had a greater impact on the films thermal conductance than the randomly oriented CNTs. The study shows that one can achieve better thermal conductance by using vertically aligned CNFs in place of randomly oriented CNTs in a polymer composite. Although no additional measures were used in this study to evenly disperse the CNTs before introducing them into the polymer, an improvement in thermal conductance is observed. CNF enhanced films demonstrate higher thermal conductances than CNT enhanced films in thicknesses less than 60 μm.

Acknowledgments

Study was conducted with funding from a USU Summer Undergraduate Research and Creative Opportunity (SURCO) Grant and a Utah State University College Engineering Undergraduate Research Program (EURP) grant. We acknowledge the support from the National Science Foundation (CMMI-1337932) and the Microscopy Core Facility at Utah State University for the SEM result. Additional lab assistance provided by the Utah State University Department of Mechanical and Aerospace Engineering.

CNF growth by DC PECVD (D.K.H.) experiments were conducted at ORNLs Center for Nanophase Materials Sciences, which is a DOE Office of Science User Facility.

Conflict of Interest

All authors declare no conflicts of interest in this paper.

References

1 Downing R, Kojasoy G (2002) Single and two-phase pressure drop characteristics in miniature helical channels. *Exp Therm Fluid Sci* 26: 535–546.

2 Jagannadham K (2012) Thermal conductivity of copper-graphene composite films synthesized by electrochemical deposition with exfoliated graphene platelets. *Metall Mater Trans B* 43: 316–324.

3 Wejrzanowski T, Grybczuk M, Chmielewski M, et al. (2016) Thermal conductivity of metal-graphene composites. *Mater Des* 99: 163–173.

4 Wejrzanowski T, Grybczuk M, Chmielewski M, et al. (2015) Heat transfer through metal-graphene interfaces. *AIP Adv* 5: 077142.

5 Han Z, Fina A (2011) Thermal conductivity of carbon nanotubes and their polymer nanocomposites: A review. *Prog Polym Sci* 36: 914–944.

6 Kuncova-Kallio J, Kallio PJ (2006) PDMS and its suitability for analytical microfluidic devices. *Engineering in Medicine and Biology Society, 2006. EMBS '06. 28th Annual International Conference of the IEEE* 2486–2489.

7 Jothimuthu P, Carroll A, Bhagat AAS (2009) Photodefinable PDMS thin films for microfabrication applications. *J Micromech Microeng* 19: 045024.

8 Yabuta T, Bescher EP, Mackenzie JD, et al. (2003) Synthesis of PDMS-based porous materials for biomedical applications. *J Sol Gel Sci Technol* 26: 1219–1222.

9 Fujii T (2001) PDMS-based microfluidic devices for biomedical applications. *Microelectron Eng* 61: 907–914.

10 Visser SA, Hergenrother RW, Cooper SL (1996) Polymers. *Biomat Sci* 59.

11 Saunders TS, Fry JS, Neuraxis, LLC, assignee. Methods and devices for cooling spinal tissue. United States patent US 8,523,930. 2013 Sep. 3.

12 Sullivan J; Neuraxis, LLC, assignee. Tissue cooling clamps and related methods. United States patent US 8,721,642. 2014 May 4.

13 Lee KL, Li Y, Guzek BJ, et al. (2015) Compact heat rejection system utilizing Integral Planar Variable Conductance Heat Pipe Radiator for space application. *Gravitational Space Res* 3.30–41.

14 Prasher R, Chiu CP (2009) Materials for Advanced Packaging. Boston: Springer US. Thermal Interface Materials, 437–458.

15 Thompson DR, Cola BA (2013) A stepped-bar apparatus for thermal resistance measurements. *J Electronic Packaging* 135.

16 Uma S, McConnell AD, Asheghi M, et al. (2001) Temperature-dependent thermal conductivity of undoped polycrystalline silicon layers. *Int J Thermophys* 22: 605–616.

17 Zhang Y, Tadigadapa S (2005) Thermal characterization of liquids and polymer films using a microcalorimeter. *Appl Phys Lett* 86.

18 Kurabayashi K, Asheghi M, Touzelbaev M, et al. (1999) Measurement of the thermal conductivity anisotropy in polyimide films. *IJT* 8: 180–191.

19 Ju YS, Kurabayashi K, Goodson KE (1999) Thermal characterization of aisotropic thin dielectric films using harmonic joule heating. *Thin Solid Films* 339: 160–164.

20 Choy CL, Yang GW, Wong YW (1997) Thermal diffusivity of polymer films by pulsed photothermal radiometry. *J Polym Sci Pol Phys* 35: 1621–1631.

21 Choy CL, Yang GW, Wong YW, et al. (1999) Elastic modulus and thermal conductivity of ultradrawn polyethylene. *J Polym Sci Pol Phys* 37: 3359–3367.

22 Eiermann K, Hellwege KH (1962) Thermal conductivity of high polymers from -180 to 90 C. *J Polym Sci* 57: 99–106.

23 Sabate N,Santander J, Gracia I, et al. (2005) Characterization of thermal conductivity in thin film multilayered membranes. *Thin Solid Films* 484: 328–333.

24 Chu DC, Touzelbaev M, Goodson KE, et al. (2001) Thermal conductivity measurements of thin-film resist. *J Vac Sci Technol* 19: 2874–2877.

25 Watabe K, Polynkin P, Mansuripur M (2005) Optical pump-and-probe test system for thermal characterization of thin metal and phase-change films. *Appl Optics* 44: 3167–3173.

26 Langer G, Hartmann J, Reichling M (1997) Thermal conductivity of thin metallic films measured by photothermal profile analysis. *Rev Sci Instrum* 68: 1510–1513.

27 Rao VV, Bapurao K, Nagaraju J, et al. (2004) Instrumentation to measure thermal contact resistance. *Meas Sci Technol* 15: 275–278.

28 Savija I, Culham JR, Yovanovich MM, et al. (2003) Review of thermal conductance models for joints incorporating enhancement materials. *J Thermophys Heat Tr* 17:43–52.

29 Kempers R, Kolodner P, Lyons A, et al. (2009) A high-precision apparatus for the characterization of thermal interface materials. *Rev Sci Instrum* 80.

30 Ralphs M, Smith B, Roberts N (2016) Technique for direct measurement of thermal conductivity of elastomers and a detailed uncertainty analysis. [Submitted].

AIMS Press